

Dilepton production from virtual bremsstrahlung induced by proton capture

D. Van Neck, A.E.L. Dieperink and O. Scholten

Kernfysisch Versneller Instituut, Zernikelaan 25, 9747 AA Groningen, The Netherlands

Abstract

Dilepton production following radiative capture of a proton on a nuclear target is studied in the Impulse Approximation. The cross section is decomposed in terms of four time-like nuclear structure functions through a longitudinal-transverse separation of the nuclear current. Using a simple PWIA model, cross sections and conversion factors are calculated for capture reactions $p + n \rightarrow d + e^+e^-$, $p + p \rightarrow {}^2\text{He} + e^+e^-$ and $p + {}^{11}\text{B} \rightarrow {}^{12}\text{C} + e^+e^-$ at proton energies of 100-200 MeV. The result is compared with a recent measurement of the conversion factor for $p + {}^{11}\text{B}$.

arXiv:nucl-th/9311023v1 24 Nov 1993

I. INTRODUCTION

The detection of dilepton pairs has been shown to be a powerful technique in heavy-ion reactions. In heavy-ion reactions at higher energies there are several sources of dileptons, (i) nucleon-nucleon bremsstrahlung, (ii) Dalitz decay of resonances and mesons, (iii) meson annihilation. The interest here lies in the study of medium effects and possible phase transitions. In order to separate the contributions from the first and the latter two mechanisms, it is important to be able to describe the cross section for the bremsstrahlung accurately. This can be done best for simple systems like $p + A$ or $p + p(n)$.

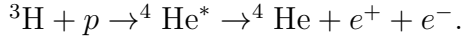
Recently it was shown [1] that detection of dilepton pairs even at relatively low energies ($E = 100$ MeV) is feasible, e.g. in the radiative capture of protons on ^{11}B . Interestingly it was found that the conversion ratio $R = \sigma(\text{dilepton})/\sigma(\text{photon})$ (at fixed photon angle) varied with excitation energy in the final nucleus.

In addition to being of interest for the general understanding of the virtual bremsstrahlung process in the nuclear medium the investigation of production of dileptons in $p + A$ is of interest for specific reasons. For example a new aspect of dilepton production (compared to real photon production) is the presence of a virtual longitudinally polarized photon. Furthermore this process contains information on the time-like nucleon form factor which is not easy to obtain otherwise.

To compute the cross section for dilepton production at lower energies (below the pion production threshold) it is extremely useful to decompose the amplitudes in longitudinal (L) and transverse (T) components which have a different dependence on the kinematic observables, analogously to the $(e, e'p)$ reaction which can be viewed as the spacelike counterpart. As a result one can (in the impulse approximation) make a separation of the cross section into transverse and longitudinal parts.

The interest in isolating the longitudinal part stems from the fact that it is assumed to correspond to a simple charge operator with a monopole (C0) component which is expected to be insensitive to exchange currents. In fact the study of the C0 component is also of

interest in related fields of physics, e.g. in muon catalyzed fusion [2]



In this paper we compute the cross section for dilepton production for the special limit of radiative capture of a proton on a nuclear target in the PWIA (Plane Wave Impulse approximation). We decompose the cross section in terms of longitudinal, transverse and interference terms. Then we express the cross-section ratio of virtual to real photons in terms of L and T conversion factors. Using a simple one-body prescription for the nucleon current we consider radiative capture for $p + n \rightarrow d + e^+e^-$, $p + n \rightarrow {}^2\text{He} + e^+e^-$ and $p + {}^{11}\text{B} \rightarrow {}^{12}\text{C} + e^+e^-$.

II. DERIVATION OF THE CROSS SECTION

We consider the reaction $p + A \rightarrow (A+1) + e^+ + e^-$ (with A an unspecified nuclear system) in the Impulse Approximation (IA). The four-momenta involved (see figure 1) will be denoted by p^μ (incoming proton), k_A^μ, k_{A+1}^μ (target and residual nuclear system), q_1^μ, q_2^μ (outgoing electron and positron). The exchanged virtual (time-like) photon has 4-momentum $Q^\mu = q_1^\mu + q_2^\mu$ and an invariant mass $M^2 = Q \cdot Q = Q_0^2 - Q^2 > 0$.

The squared amplitude for this process in the one-photon approximation is written as

$$|\mathcal{T}|^2 = \frac{e^4}{(Q \cdot Q)^2} |j \cdot J|^2 = \frac{e^4}{M^4} J_\mu^* J_\nu L^{\mu\nu}, \quad (1)$$

with j^μ the lepton and J^μ the nuclear current. After summation over the e^+e^- polarizations, the lepton tensor is equal to (see e.g. [3]):

$$\begin{aligned} L^{\mu\nu} &= \frac{1}{4m_e^2} \text{Trace}((\not{q}_2 - m_e)\gamma^\mu(\not{q}_1 + m_e)\gamma^\nu) \\ &= \frac{1}{m_e^2} (q_1^\mu q_2^\nu + q_2^\mu q_1^\nu - g^{\mu\nu}(q_1 \cdot q_2 + m_e^2)) \\ &= \frac{1}{2m_e^2} (Q^\mu Q^\nu - q^\mu q^\nu - M^2 g^{\mu\nu}), \end{aligned} \quad (2)$$

with $q^\mu = q_1^\mu - q_2^\mu$ the relative e^+e^- momentum. The appearance of a negative energy projection operator ($m_e - \not{q}_2$) in eq. (2) is the only difference with the corresponding expression in (e, e') scattering.

Taking current conservation ($J \cdot Q = 0$) into account, the invariant amplitude can be expressed as:

$$|\mathcal{T}|^2 = \frac{e^4}{M^4} \frac{1}{2m_e^2} \left(-|J \cdot q|^2 - M^2 J^* \cdot J \right). \quad (3)$$

It is our aim to express the cross section for (p, e^+e^-) , analogously to the well-known LT (longitudinal-transverse) decomposition for the $(e, e'p)$ process [4,5], in terms of four independent structure functions.

We introduce the L and T components of the spatial part of the nuclear current:

$$\vec{J} = \vec{J}_L + \vec{J}_T, \quad (4)$$

with

$$\vec{J}_L = \frac{(\vec{J} \cdot \vec{Q})}{Q^2} \vec{Q}. \quad (5)$$

Furthermore we decompose \vec{J}_T in two transverse directions: $\vec{J}_T = J_{+1} \vec{e}_{+1}^* + J_{-1} \vec{e}_{-1}^*$, with $\vec{e}_{\pm 1} = \mp \frac{1}{\sqrt{2}} (\vec{e}_x \pm i \vec{e}_y)$ defined in the reference system with the z -axis along \vec{Q} and the y -axis along $\vec{Q} \times \vec{p}$ (see figure 2).

The LT separation of the terms in eq. (3) reads as:

$$J^* \cdot J = -\frac{M^2}{Q_0^2} |J_L|^2 - |J_T|^2 \quad (6)$$

$$J \cdot q = -\frac{M^2}{Q_0^2} q \cos \theta_q J_L + \frac{1}{\sqrt{2}} q \sin \theta_q (J_{+1} e^{-i\varphi_q} - J_{-1} e^{i\varphi_q}), \quad (7)$$

in terms of the solid angle $\Omega_q = (\theta_q, \varphi_q)$ of \vec{q} in the reference frame of figure 2. Note that we have used the continuity equation

$$Q J_L = Q_0 J_0 \quad (8)$$

to replace the charge density J_0 by the longitudinal component J_L of the nuclear current.

The reason for this will be explained in section III.

The differential $A(p, e^+e^-)A + 1$ cross section reads as:

$$d\sigma(p, e^+e^-) = \frac{d\vec{q}_1 d\vec{q}_2 m_e^2}{(2\pi)^6 (q_1)_0 (q_2)_0} \frac{d\vec{k}_{A+1}}{(2\pi)^3} \frac{(2\pi)^4 \delta^{(4)}(k_{A+1} + q_1 + q_2 - p - k_A)}{4\sqrt{(p \cdot k_A)^2 - m^2 m_A^2}} |\mathcal{T}|^2. \quad (9)$$

We will evaluate this cross section in the CM frame. Introducing the invariant mass M and momentum \vec{Q} of the virtual photon as new variables, the cross section (9) can be written as:

$$d\sigma(p, e^+e^-) = \frac{1}{64\pi^2 s} \frac{Q}{p} P_{e^+e^-} |\mathcal{T}|^2 d\Omega dM^2, \quad (10)$$

with \sqrt{s} the total CM energy, Ω the solid angle of \vec{Q} in the CM frame, and $P_{e^+e^-}$ the phase space factor for the decay of the virtual photon into the e^+e^- pair. The latter quantity is given by:

$$P_{e^+e^-} = \int \frac{m_e^2 d\vec{q}_1 d\vec{q}_2 \delta^{(4)}(Q - q_1 - q_2)}{(2\pi)^3 (q_1)_0 (q_2)_0}. \quad (11)$$

It is convenient to evaluate $P_{e^+e^-}$ in the rest frame of the decaying virtual photon:

$$P_{e^+e^-} = \frac{m_e^2}{(2\pi)^3} \frac{u}{2} d\Omega'_q, \quad (12)$$

with $\Omega'_q = (\theta'_q, \varphi'_q)$ the solid angle of the relative e^+e^- momentum in the rest frame of the virtual photon and $u = \sqrt{1 - 4m_e^2/M^2}$.

The relation between Ω_q and Ω'_q can be found by boosting the relative e^+e^- momentum along \vec{Q} with velocity Q/Q_0 :

$$\begin{aligned} \varphi'_q &= \varphi_q, \\ uM \cos \theta'_q &= \frac{Q_0}{M} q \cos \theta_q - \frac{Q}{M} q_0 = \frac{qM}{Q_0} \cos \theta_q, \\ uM \sin \theta'_q &= q \sin \theta_q. \end{aligned} \quad (13)$$

The angle φ'_q represents the angle between the plane of (\vec{p}, \vec{Q}) and that of the dilepton pair. The angle θ'_q is related to the asymmetry in the energies of the e^+e^- pair, since

$$\cos \theta'_q = \frac{(q_1)_0 - (q_2)_0}{uQ}, \quad (14)$$

and plays a similar role as the electron scattering angle in the $(e, e'p)$ reaction.

This becomes evident if we write the CM cross section after LT decomposition, using eqs. (6-13) (α is the fine-structure constant):

$$\begin{aligned} \frac{d\sigma(p, e^+e^-)}{d\Omega dM d\Omega'_q} &= \frac{\alpha^2}{64\pi^2 s} \frac{Q}{p} \frac{u}{M\pi} \left\{ (1 - u^2 \cos^2 \theta'_q) W_L \right. \\ &\quad + (1 - \frac{u^2}{2} \sin^2 \theta'_q) W_T \\ &\quad + \frac{u^2}{2} \sin^2 \theta'_q \cos(2\varphi'_q) W_{TT} \\ &\quad \left. + u^2 \sqrt{2} \sin(2\theta'_q) \cos \varphi'_q W_{LT} \right\}. \end{aligned} \quad (15)$$

The nuclear structure functions W_i are given by:

$$\begin{aligned} W_L(p, Q, \theta, M) &= \frac{M^2}{Q_0^2} |J_L|^2 \\ W_T(p, Q, \theta, M) &= |J_T|^2 \\ W_{TT}(p, Q, \theta, M) &= 2\Re(J_{+1} J_{-1}^*) \\ W_{LT}(p, Q, \theta, M) &= \frac{M}{Q_0} 2\Re(J_L J_{+1}^* - J_L J_{-1}^*). \end{aligned} \quad (16)$$

The different structure functions can be experimentally separated through the dependence on the dilepton angles θ'_q and φ'_q of each term in (15).

Based on eq. (15) one can derive various integrated cross sections. Integration over the out-of-plane angle φ'_q of the e^+e^- pair makes the LT and TT interference terms (the last two terms in eq. (15)) vanish. A further integration over the asymmetry $\cos \theta'_q$ of the pair leads to

$$\frac{d\sigma(p, e^+e^-)}{d\Omega dM} = \frac{\alpha^2}{64\pi^2 s} \frac{Q}{p} \frac{4}{M} u \left(1 - \frac{u^2}{3}\right) (W_L + W_T). \quad (17)$$

In many situations there is experimental information on the (p, γ) cross sections for real photons. Therefore it is of interest to introduce the conversion factor $R(M, \theta)$, defined as the ratio of the cross sections for emission of a virtual and a real photon in the same direction Ω :

$$R(M, \theta) = \frac{d\sigma(p, e^+e^-)}{d\Omega dM} / \frac{d\sigma(p, \gamma)}{d\Omega} = R_L(M, \theta) + R_T(M, \theta) \quad (18)$$

The CM cross section for the $A(p, \gamma)A + 1$ process in the denominator of eq. (18) is given by

$$\frac{d\sigma(p, \gamma)}{d\Omega} = \frac{\alpha}{64\pi^2 s} \frac{k}{p} 4\pi |J_T|^2, \quad (19)$$

with \vec{k} the momentum of the real photon. The longitudinal and transverse conversion factors become ($i=L, T$):

$$R_i(M, \theta) = \frac{Q}{k} \frac{\alpha}{\pi} u \left(1 - \frac{u^2}{3}\right) \frac{1}{M} \frac{W_i(p, Q, \theta, M)}{W_T(p, k, \theta, 0)}. \quad (20)$$

In the following we will focus on properties of the conversion factors R_i . In particular we will explore its dependence on M, θ and nuclear structure.

III. THE NUCLEAR CURRENT IN PWIA

For this purpose we will use the non-relativistic one-body current operator, which has the form:

$$\langle \hat{J}_0(\vec{Q}, M) \rangle = G_E(M^2) \quad (21)$$

$$\langle \hat{\vec{J}}(\vec{Q}, M) \rangle = \frac{1}{2m} \left(G_E(M^2)(\vec{p}_i + \vec{p}_f) + G_M(M^2)\vec{Q} \times i\vec{\sigma} \right), \quad (22)$$

taken between momentum eigenstates \vec{p}_i and \vec{p}_f , with $\vec{Q} = \vec{p}_i - \vec{p}_f$.

The nucleon mass is m and G_E, G_M are the Sachs nucleon form factors in the time-like region. For the relatively small values of M ($M < 100$ MeV) that we will consider we use the continuation in the time-like region of the dipole fit for the nuclear form factors. We neglect the off-shellness of the captured proton.

The nuclear transition current in eq. (3) is then given by

$$\vec{J}(\vec{Q}, M) = \langle A + 1 | \hat{\vec{J}}(\vec{Q}, M) | A, \vec{p} m_s \rangle, \quad (23)$$

with $|A \rangle$ and $|A + 1 \rangle$ non-relativistic wave functions of the target and residual nucleus. Note that the use of non-relativistic wave functions introduces an extra normalization factor $(2k_A^0)(2k_{A+1}^0)(2p^0)$ in our expressions (15-19) for the cross section.

In contrast to the conventional PWIA treatment of the $(e, e'p)$ reaction, where J_L is eliminated, we retain the longitudinal component J_L of the nuclear current instead of the charge density J_0 . Both are in principle related via the continuity equation (8) if the initial and final state are true eigenstates of the nuclear hamiltonian (and if the used current and charge operators are consistent with the same hamiltonian). It is known [6–8] that, due to the non-orthogonality of the bound-state wave function and the plane-wave scattering state, the PWIA treatment of the transition charge density leads to incorrect results in the region of small three-momentum transfer Q (even for large proton energies), since in PWIA $J_0(Q \rightarrow 0) \neq 0$. In the (p, e^+e^-) reaction the longitudinal response favours large invariant masses of the virtual photon, which means small three-momentum transfer $Q = \sqrt{Q_0^2 - M^2}$. The use of J_L at least guarantees the correct small- Q , large- p behaviour of the longitudinal nuclear response, as shown by the analysis of Amado et al. [7].

A. Factorized form of the current for medium and heavy nuclei

If we make the assumption (similar to the IA treatment of the $(e, e'p)$ reaction) that the incoming proton emits the photon, the matrix element of the current between initial and final nuclear states (eq.(23)) becomes (neglecting CM motion):

$$\vec{J}(\vec{Q}, M) = \int d\vec{p}_i \int d\vec{p}_f \int d\sigma \varphi^*(\vec{p}_f, \sigma) \delta(\vec{Q} - \vec{p}_i + \vec{p}_f) \langle \hat{J}(\vec{Q}, M) \rangle \psi_{\vec{p}m_s}(\vec{p}_i, \sigma), \quad (24)$$

with φ the overlap function between $|A\rangle$ and $|A+1\rangle$ and $\psi_{\vec{p}}$ the wave function of the incident proton in momentum space.

Taking a plane-wave description for the incident proton, $\psi_{\vec{p}}$ reduces to a delta-function, and the current becomes:

$$\vec{J}(\vec{Q}, M) = \frac{1}{2m} \int d\sigma \varphi^*(\vec{p} - \vec{Q}, \sigma) \left(G_E(2\vec{p} - \vec{Q}) + G_M \vec{Q} \times i\vec{\sigma} \right) \chi_{m_s}(\sigma). \quad (25)$$

It can be shown, by a similar analysis as in the case of the $(e, e'p)$ process [5], that after averaging over the spins of the incident proton and target nucleus and summing over the spin

of the residual nucleus, the four structure functions in PWIA have a common factor in which the dependence on the nuclear structure of the target and residual nucleus is contained. The structure functions in eq. (16) become, after this spin summation:

$$W_L = \frac{1}{2(2J_A + 1)} \frac{M^2}{Q_0^2} \frac{(2\pi)^3}{(2m)^2} G_E^2 (2p \cos \theta - Q)^2 S(|\vec{p} - \vec{Q}|) \quad (26)$$

$$W_T = \frac{1}{2(2J_A + 1)} \frac{(2\pi)^3}{(2m)^2} (G_E^2 4p^2 \sin^2 \theta + 2G_M^2 Q^2) S(|\vec{p} - \vec{Q}|) \quad (27)$$

$$W_{LT} = \frac{1}{2(2J_A + 1)} \frac{M}{Q_0} \frac{(2\pi)^3}{(2m)^2} G_E^2 (-4\sqrt{2}) p \sin \theta (2p \cos \theta - Q) S(|\vec{p} - \vec{Q}|) \quad (28)$$

$$W_{TT} = \frac{1}{2(2J_A + 1)} \frac{(2\pi)^3}{(2m)^2} G_E^2 (-4)p^2 \sin^2 \theta S(|\vec{p} - \vec{Q}|). \quad (29)$$

As a result, the total cross-section is also factorized into a kinematical part and a nuclear structure part.

The common function S is related to the spectral function for addition of a proton to the target nucleus in its ground state. Its explicit form reads as:

$$S(k) = \frac{1}{4\pi} \sum_{lj} | \langle J_{A+1} || c_{lj}^+(k) || J_A \rangle |^2, \quad (30)$$

with the reduced matrix element defined as in [9]. If the ground state of the target can be described as a pure one-hole state h with respect to a spherical closed-shell residual nucleus, we have

$$S(k) = \frac{2j_h + 1}{4\pi} |\phi_h(k)|^2, \quad (31)$$

with the hole orbital $\phi_h(k)$ normalized as

$$\int dk k^2 |\phi_h(k)|^2 = 1. \quad (32)$$

B. Nuclear current for the $A = 2$ system

For two-body systems, CM motion can of course be treated exactly. We now also take photon emission by both nucleons into account.

For the purpose of comparing $p + n$ and $p + p$ capture we first assume a pure $l = 0$ state ϕ_0 (no D-state admixture) as the spatial part of the internal deuteron wavefunction. For the quasi-bound ${}^2\text{He}$ system we take the same spatial wavefunction ϕ_0 , but replace the spin triplet of the deuteron by a singlet state. We used the $l = 0$ part of the parametrization of the deuteron wave function by Machleidt et al. (table 11 in [10]).

It is interesting to study the effects of the antisymmetrization in case of identical nucleons. If we couple the spins of the two-nucleon initial state to S' , and denote by S the spin of the final bound state, the nuclear current is given by

$$\begin{aligned}
J_L &= \frac{1}{2m} \left(2p \cos \theta (G_E^{(1)} \phi_0^{(1)} - G_E^{(2)} \phi_0^{(2)}) - Q (G_E^{(1)} \phi_0^{(1)} + G_E^{(2)} \phi_0^{(2)}) \right) \delta_{SS'} \delta_{M_S M_{S'}} \\
J_{\pm 1} &= \mp \frac{1}{2m} \left(\sqrt{2} p \sin \theta (G_E^{(1)} \phi_0^{(1)} - G_E^{(2)} \phi_0^{(2)}) \delta_{SS'} \delta_{M_S M_{S'}} \right. \\
&\quad \left. - Q (1 - \delta_{S0} \delta_{S'0}) S_{\pm} (G_M^{(1)} \phi_0^{(1)} + (-1)^{S+S'} G_M^{(2)} \phi_0^{(2)}) \right), \tag{33}
\end{aligned}$$

with $\phi_0^{(i)} = \phi_0(k_i)$ and $\vec{k}_1 = \vec{p} - \vec{Q}/2$, $\vec{k}_2 = \vec{p} + \vec{Q}/2$. The spin factor S_{\pm} is given by:

$$S_{\pm}(SM_S, S'M_{S'}) = \langle \frac{1}{2} \frac{1}{2} S' M_{S'} | \sigma_{\pm 1}(1) | \frac{1}{2} \frac{1}{2} SM_S \rangle. \tag{34}$$

It is clear from eq. (33) that interference effects can occur between the contributions from the two nucleons to the current. This will be further discussed in section IV A.

For the case of $p + n$ capture we will also give results with a more realistic treatment of the deuteron wave function in which the D-state is included. The expressions for the nuclear structure functions, as defined in eq. (16), then become (after averaging over initial and summing over final spin):

$$\begin{aligned}
W_L &= \frac{(2\pi)^3}{4} \left(\frac{3}{4\pi} \sum_i \sum_l |C_l^{(i)}|^2 + \frac{3}{2\pi} \sum_l C_l^{(1)} C_l^{(2)} P_l(\cos \omega_{12}) \right) \\
W_T &= \frac{(2\pi)^3}{4} \left(\frac{3}{2\pi} \sum_i \sum_l (|E_l^{(i)}|^2 + |M_l^{(i)}|^2) \right. \\
&\quad \left. + \frac{1}{\pi} \sum_l (3E_l^{(1)} E_l^{(2)} + M_l^{(1)} M_l^{(2)}) P_l(\cos \omega_{12}) \right. \\
&\quad \left. - \frac{\sqrt{2}}{\pi} (M_0^{(1)} M_2^{(2)} P_2(\cos \theta_2) + M_2^{(1)} M_0^{(2)} P_2(\cos \theta_1)) \right. \\
&\quad \left. - \frac{2}{5} \sqrt{2} \sqrt{7} M_2^{(1)} M_2^{(2)} [Y_2(\Omega_1) \otimes Y_2(\Omega_2)]_0^2 \right) \tag{35}
\end{aligned}$$

$$\begin{aligned}
& -\frac{12}{\sqrt{10}}(E_2^{(1)}M_2^{(2)} - M_2^{(1)}E_2^{(2)})[Y_2(\Omega_1) \otimes Y_2(\Omega_2)]_1^1 \Big) \tag{36} \\
W_{TT} = & \frac{(2\pi)^3}{4} \left(-\frac{3}{4\pi} \sum_i \sum_l |E_l^{(i)}|^2 - \frac{3}{2\pi} \sum_l E_l^{(1)} E_l^{(2)} P_l(\cos \omega_{12}) \right. \\
& + \frac{12}{\sqrt{15}} \frac{1}{\sqrt{4\pi}} (M_0^{(1)} M_2^{(2)} Y_{22}(\Omega_2) + M_2^{(1)} M_0^{(2)} Y_{22}(\Omega_1)) \\
& + \frac{6\sqrt{7}}{5\sqrt{3}} M_2^{(1)} M_2^{(2)} [Y_2(\Omega_1) \otimes Y_2(\Omega_2)]_2^2 \\
& \left. + \frac{6}{\sqrt{10}}(E_2^{(1)}M_2^{(2)} - M_2^{(1)}E_2^{(2)})[Y_2(\Omega_1) \otimes Y_2(\Omega_2)]_1^1 \right) \tag{37} \\
W_{LT} = & \frac{(2\pi)^3}{4} \left(\frac{3}{4\pi} \sum_i \sum_l E_l^{(i)} C_l^{(i)} \right. \\
& + \frac{3}{4\pi} \sum_l (C_l^{(1)} E_l^{(2)} + E_l^{(1)} C_l^{(2)}) P_l(\cos \omega_{12}) \\
& \left. - \frac{3}{\sqrt{10}}(C_2^{(1)}M_2^{(2)} - M_2^{(1)}C_2^{(2)})[Y_2(\Omega_1) \otimes Y_2(\Omega_2)]_1^1 \right), \tag{38}
\end{aligned}$$

with Ω_i the solid angle of \vec{k}_i and ω_{12} the angle between \vec{k}_1 and \vec{k}_2 . The quantities C, E, M are defined as (the upper and lower signs correspond to $i = 1, 2$ respectively):

$$\begin{aligned}
C_l^{(i)} &= \frac{1}{2m} (\pm 2p \cos \theta - Q) G_E^{(i)} \phi_l^{(i)} \\
E_l^{(i)} &= \frac{1}{2m} (\mp \sqrt{2} p \sin \theta) G_E^{(i)} \phi_l^{(i)} \\
M_l^{(i)} &= \frac{1}{2m} Q G_M^{(i)} \phi_l^{(i)}. \tag{39}
\end{aligned}$$

They are associated with the longitudinal (C) and transverse (E) part of the convection current, and with the magnetic (M) current.

The deuteron wave function was normalized as:

$$\sum_{l=0,2} \int dk k^2 |\phi_l(k)|^2 = 1. \tag{40}$$

The structure functions corresponding to the nuclear current in eq. (33) (with $S = 1$) can be obtained from eqs. (35-38) by omitting the terms with $l = 2$.

IV. APPLICATIONS

A. Results for the $A = 2$ system

We first compare e^+e^- production for pp and pn capture into a bound S-state (see section III) for 200 MeV incident protons. This corresponds to virtual photons with invariant mass up to about 100 MeV.

In figure 3 we show the (p, e^+e^-) cross section as a function of the invariant mass. The transverse part is sharply peaked at low invariant masses, due to the phase-space factor Q/M in eq. (17). Therefore its angular dependence will be similar to that of the (p, γ) cross section. The longitudinal part, on the other hand, gets its main contributions at intermediate and high invariant masses, due to the additional factor M^2/Q_0^2 for W_L in eq. (16).

We see that the pp cross section is overall smaller than the pn , in both the transverse and longitudinal part.

The angular dependence of the (p, e^+e^-) cross section is shown in figure 4. Note that the cross section for the pp system is symmetric around a scattering angle of 90° . The transverse part has a similar behaviour as the (p, γ) cross section for both pp and pn systems. One sees that at forward angles the transverse (p, e^+e^-) cross section for the pp system is much smaller than that for the pn system (the same holds for the (p, γ) cross section). This can be understood from the structure of the nuclear currents in eq. (33). In the case of identical particles 1 and 2, we have $S = 0$ for the final state. As noted in [11], the magnetic current then requires $S' = 1$ for the initial state, and destructive interference will occur. The same also holds for the part of the convection current proportional to \vec{p} . Therefore the transverse part of the cross section is severely suppressed. It even has a sharp zero at 90° in this simple model for the hadron current, though this feature will be eliminated by higher order terms in the non-relativistic expansion of the current operator (such as the relativistic spin correction [11]), and distortion effects.

One would expect the longitudinal part of the (p, e^+e^-) cross section to become dominant for pp capture, because the charge density operator is unaffected by interference effects.

However, the PWIA treatment of the transition charge density is incorrect at low three-momentum of the photon [7], since in that case orthogonality of initial and final state strongly suppresses the longitudinal response. In a PWIA approach one should preferably use the longitudinal current instead of the charge density. By inspecting eq. (33) it is clear that the part of the longitudinal current proportional to $p(G_E^{(1)}\phi_0^{(1)} - G_E^{(2)}\phi_0^{(2)})$ interferes destructively, which leads to a further suppression. As a result the longitudinal cross section is also for the pp system smaller than the transverse cross section, except in the region around 90° where the transverse response vanishes in the present model.

This is also reflected in the conversion ratios (integrated over invariant mass), which are shown in figure 5. The conversion ratio is expected to be about α because of the second electromagnetic interaction vertex. The calculated values are indeed of the order of α , but we see some non-trivial structure. The conversion ratios may thus be an interesting observable to gain insight in the electromagnetic response of nuclear systems. For both the pn and pp system, R_T has little angular dependence, showing that the transverse (p, e^+e^-) response follows roughly the real photon response.

The longitudinal conversion ratio R_L is smaller than R_T and peaked at forward and backward scattering angles in case of pn . The same holds for the pp system, where additionally an enhancement of R_L is observed near 90° , where the transverse one-body current vanishes in the present model.

From now on the results are based on the full deuteron wave function (D-state included) of [10]. Figure 6 shows the energy dependence of the conversion factors for the case of pn capture. Naively one would expect, on the basis of diminishing phase space for the virtual photon, that both longitudinal and transverse conversion ratios should decrease with decreasing proton energy. This is true only at small incident proton energies, however. The longitudinal R_L first increases and goes (in this PWIA model) to a maximum at $T=10$ MeV before decreasing.

Figures 7 and 8 contain the four structure functions as a function of invariant mass, for two angles. Their contributions to the nuclear current are of comparable magnitude as the

direct L and T terms. In order to investigate the sensitivity to the nuclear structure, we also plotted the result for another parametrization of the deuteron wave function (table 13 in [10]), which has a different ratio of S-state component to D-state component in the relevant momentum region. The sensitivity is about the same in all four structure functions, and drops out in both conversion ratios.

B. Results for ^{12}C

For capture to the ^{12}C groundstate the spectral function reduces to the squared $1p3/2$ single-particle wave function in momentum space. Since the (p, γ) cross section in PWIA has (unphysical) zeros, and thus gives rise to infinities in the conversion ratios, we replace the pure PWIA momentum distribution by corresponding DWIA momentum distributions taken directly from $^{11}\text{B}(p, \gamma)$ calculations [12,13] by dividing out the PWIA kinematical factor. In this way we can also include in an approximative way the effect of ISI (initial state interactions) on the conversion ratios, which are shown in figure 9. The incident proton energy was 98 MeV. The first two momentum distributions (labeled HF and RPA) were taken from [12]. The labels refer to the treatment of the ISI: in HF the incident proton was described as a scattering state of the mean field, in RPA the ISI are treated through an RPA description of the $^{11}\text{B} + p$ system. The latter was able to give a fair description of the (p, γ) cross section. The same holds for the third momentum distribution (labeled $np - nh$), taken from the continuum shell model calculation in [13]. The behaviour of the conversion factors is quite similar to the case of pn capture. Sizeable differences can be noted between the three approximations, which can be related to the different slope of the distorted momentum distributions at large momenta.

In the literature experimental values of the conversion factor for $^{11}\text{B}(p, e^+e^-)$ have been reported by the Uppsala group [1]. However, the quoted experimental values are much larger than any of the DWIA calculations presented. At present we have no explanation for this. It is unlikely that this can be attributed to the time-like nucleon form factor, which has a

negligible variation in the region of the invariant mass of the virtual photon that we are considering here (less than 3% on the current matrix elements).

V. SUMMARY AND DISCUSSION

In this paper we have derived the cross section for dilepton production in radiative capture of protons on nuclei. As an illustration we have computed the cross section for $A = 1$ and $A = 11$ targets in the PWIA. Analogously to the $(e, e'p)$ reaction, where the exchanged photon is space-like, we have decomposed the cross section for (p, e^+e^-) into four independent structure functions which can be experimentally separated by varying the kinematic variables.

In order to see whether the virtual photon process contains new information compared to the (p, γ) reaction we have studied the dependence of the conversion factors (i.e. the ratio of the virtual to real photon cross sections) on invariant mass of the e^+e^- pair, scattering angle of the photon, and proton energy.

We found that the longitudinal conversion factor (which represents a new degree of freedom since it contains a monopole contribution) peaks at rather large invariant mass M and is small compared to the transverse one which is sharply peaked at small values of M (and is of order α).

There appears to be some sensitivity of the conversion factors to the details of the nuclear structure (contained in the vertex function) for the case of $p + {}^{11}\text{B} \rightarrow {}^{12}\text{C}(g.s.) + e^+e^-$. The preliminary data from Uppsala do not agree with our calculations.

A unique feature of the dilepton production is that it allows one to study the nucleon form factor in the (unphysical) time-like region. However, for the momentum transfer range considered here we found only a small effect (less than 3%).

In future work we will extend the present PWIA treatment to include initial state interactions and exchange currents. From the present investigation it appears that orthogonalization of the plane wave on the final bound state represents an important correction when

the matrix elements of the charge operator are considered because of the small value of the momentum transfer.

Finally we wish to extend the formalism to the more general case of virtual bremsstrahlung in $p + A$ reactions, which is of interest to understand the NN contribution to dilepton production at higher energies.

The authors thank Dr. B. Höistad for his interest in this work, and N. Kalantar-Nayestanaki, J. Bacelar and H. Wilschut for useful discussions.

REFERENCES

- [1] B. Höistad, S. Isaksson, E. Nilsson, J. Thun, G.S. Adams, C. Landberg, T.B. Bright and S.R. Cotanch, Nucl. Phys. **A 553** (1993) 543c
- [2] L. Bogdanova and V. Markushin, Nucl. Phys. **A 508** (1990) 29c
- [3] C. Itzykson and J.-B. Zuber, Quantum Field Theory, (McGraw-Hill, New York, 1985)
- [4] C. Ciofi degli Atti, Prog. Part. Nucl. Phys. **3** (1980) 163
- [5] S. Frullani and J. Mougey, Adv. Nucl. Phys. **14** (1984) 1
- [6] F. Cannata, J.P. Dedonder and S.A. Gurvitz, Phys. Rev. **C 27** (1983) 1697
- [7] R.D. Amado, F. Cannata and J.P. Dedonder, Phys. Rev. **C 31** (1985) 162
- [8] C.Y. Cheung, S.A. Gurvitz and A.S. Rinat, Phys. Rev. **C 32** (1985) 1990
- [9] A. de Shalit and I. Talmi, Nuclear Shell Theory (Academic Press, New York, 1963)
- [10] R. Machleidt, K. Holinde and C. Elster, Phys. Rep. **149** (1987) 1
- [11] V. Herrmann and K. Nakayama, Phys. Rev. **C 46** (1992) 2199
- [12] J. Ryckebusch, M. Waroquier, K. Heyde, J. Moreau and D. Ryckbosch, Nucl. Phys. **A 476** (1988) 237
J. Ryckebusch, Inst. Nucl. Phys., Gent, Annual Report 1992
- [13] B. Höistad, E. Nilsson, J. Thun, S. Dahlgren, S. Isaksson, G.S. Adams, C. Landberg, T.B. Bright and S.R. Cotanch, Phys. Lett. **B 276** (1992)294

FIGURES

FIG. 1. Kinematical variables for the $A(p, e^+e^-)A + 1$ reaction in the Impulse Approximation.

FIG. 2. Geometry of the $A(p, e^+e^-)A + 1$ reaction in the CM frame.

FIG. 3. The (p, e^+e^-) cross section (see eq. (17)), integrated over Ω , as a function of the invariant mass M of the virtual photon. The longitudinal (L) and transverse (T) parts are shown separately. Full line: pn capture. Dashed line: pp capture. Both cross sections have been divided by the total (integrated over Ω) $n(p, \gamma)d$ cross section of eq. (19). The incident proton energy is 200 MeV.

FIG. 4. The (p, γ) cross section (labeled γ) of eq. (19) and the (p, e^+e^-) cross section of eq. (17) (integrated over M), as a function of the CM scattering angle θ of the virtual photon. The longitudinal (L) and transverse (T) parts of the (p, e^+e^-) cross section are shown separately. Full line: pn capture. Dashed line: pp capture. Both cross sections have been divided by the $n(p, \gamma)d$ cross section at $\theta = 0^\circ$. The incident proton energy is 200 MeV.

FIG. 5. Longitudinal (L) and transverse (T) conversion factors $R_i(\theta) = \int dM R_i(\theta, M)$ (see eq. (18)), as a function of the CM scattering angle θ of the photon. Full line: pn capture. Dashed line: pp capture. The conversion factors are divided by the fine-structure constant α . The incident proton energy is 200 MeV.

FIG. 6. Longitudinal (L) and transverse (T) conversion factors $R_i(\theta) = \int dM R_i(\theta, M)$ for pn capture, for three energies of the incident proton. The D-state component in the deuteron wave function is taken into account. Full, short-dashed and long-dashed lines correspond to incident proton energies of 100, 150 and 200 MeV.

FIG. 7. The four nuclear structure functions $W_i(\theta, M)$ (see eqs. (35-38)) for the $n(p, e^+e^-)d$ reaction at an incident proton energy of 200 MeV and CM scattering angle of $\theta = 5^\circ$, as a function of the invariant mass of the virtual photon. The D-state component in the deuteron wave function is taken into account. Two parametrizations of the deuteron wave function are compared. Full line: Full (energy dependent) model of ref. [10]. Dashed line: energy independent model of ref. [10].

FIG. 8. Same as figure 7, for $\theta = 45^\circ$.

FIG. 9. Longitudinal (L) and transverse (T) conversion factor $R_i(\theta) = \int dM R_i(\theta, M)$ for the reaction $p + {}^{11}\text{B} \rightarrow {}^{12}\text{C}(g.s.) + e^+ + e^-$, at an incident proton energy of 98 MeV. Three theoretical distorted-wave momentum distributions [12,13] are compared (see text): RPA (full line), HF (short-dashed line) and $np - nh$ (long-dashed line). The experimental points are taken from [1]. They should be compared to the transverse conversion factor only, because of the limitation to small invariant masses (up to about 10 MeV) in this experiment. The conversion factors are divided by the fine-structure constant α .